Cancer Science
Japanese Cancer Association JCA
Open Access

Flumatinib, a selective inhibitor of BCR-ABL/PDGFR/KIT, effectively overcomes drug resistance of certain KIT mutants

Jie Zhao, Haitian Quan, Yongping Xu, Xiangqian Kong, Lu Jin and Liguang Lou

Shanghai Institute of Materia Medica, Chinese Academy of Sciences, Shanghai, China

Key words
Drug resistance, flumatinib, gastrointestinal stromal tumors, imatinib mesylate, sunitinib malate

Correspondence
Liguang Lou, Shanghai Institute of Materia Medica, Chinese Academy of Sciences, 555 Zuchongzhi Road, Shanghai 201203, China.
Tel: +86-21-5080-6056; Fax: 86-21-5080-7088;
E-mail: lglou@mail.shcnc.ac.cn

Funding information
National Natural Science Foundation of China (Y201181042 and 81273546). National Science and Technology Major Project (2013ZX09102008 and 2013ZX09402102-001-004).

Received August 21, 2013; Revised October 22, 2013; Accepted November 5, 2013

Cancer Sci **105** (2014) 117–125

doi: 10.1111/cas.12320

Activating mutations in KIT have been associated with gastrointestinal stromal tumors (GISTs). The tyrosine kinase inhibitor imatinib mesylate has revolutionized the treatment of GISTs. Unfortunately, primary or acquired resistance to imatinib does occur in GISTs and forms a major problem. Although sunitinib malate, a multi-kinase inhibitor, has shown effectiveness against imatinib-resistant GISTs, recent studies have indicated that some imatinib-resistant GISTs harboring secondary mutations in the KIT activation loop were also resistant to sunitinib. Therefore, new drugs capable of overcoming the dual drug resistance of GISTs probably have potential clinical utility. In this study, we investigated the efficacy of flumatinib, an inhibitor of BCR-ABL/PDGFR/KIT, against 32D cells transformed by various KIT mutants and evaluated its potency to overcome the drug resistance of certain mutants. Interestingly, our *in vitro* study revealed that flumatinib effectively overcame the drug resistance of certain KIT mutants with activation loop mutations (i.e., D820G, N822K, Y823D, and A829P). Our *in vivo* study consistently suggested that flumatinib had superior efficacy compared with imatinib or sunitinib against 32D cells with the secondary mutation Y823D. Molecular modeling of flumatinib docked to the KIT kinase domain suggested a special mechanism underlying the capability of flumatinib to overcome the drug-resistance conferred by activation loop mutations. These findings suggest that flumatinib could be a promising therapeutic agent against GISTs resistant to both imatinib and sunitinib because of secondary mutations in the activation loop.

Also known as stem cell factor receptor (SCFR) or CD117, KIT is a member of the class III transmembrane receptor tyrosine kinases. Gain-of-function mutations in KIT, causing ligand-independent and constitutive activation of the receptor, have been associated with GISTs,[1–3] SM,[4,5] AML,[6,7] germ cell tumors,[8] and melanoma.[9]

The pathogenesis of most GISTs (more than 80%) results from activating mutations of KIT.[10,11] Exons 9 and 11 are the most common sites of KIT mutation in GISTs (approximately 15% and 70% of tumors, respectively).[10,11] Imatinib mesylate (Gleevec, formerly STI571; Novartis Pharmaceuticals, Basel, Switzerland) is efficacious in the majority of patients with GIST harboring KIT mutation. However, the responsiveness of GISTs to imatinib varies by primary KIT mutational status; GISTs with exon 11 mutations are more sensitive than those with exon 9 mutations.[10,11] The KIT-positive GISTs initially responsive to imatinib usually develop drug resistance during long-term treatment through acquisition of secondary mutations in the kinase domain; secondary mutations are common in GISTs that show acquired resistance, but not in those that show primary resistance.[12,13] Those mutations causing acquired imatinib resistance are usually located in the drug/ATP binding pocket or in the activation loop of the kinase domain.[12–14] Sunitinib malate (Sutent, formerly SU11248; Pfizer Pharmaceuticals, New York, NY), another KIT inhibitor, has been shown to have clinical benefit in some patients with imatinib-resistant or imatinib-intolerant GIST and has been approved by the U.S. Food and Drug Administration for treatment of imatinib-resistant GISTs.[15,16] However, recent *in vitro* and *in vivo* studies have shown that sunitinib can only effectively inhibit imatinib-resistant KIT mutants containing primary mutations in exon 9 or secondary mutations in the drug/ATP binding pocket (encoded by exons 13 and 14), but not those harboring secondary mutations in the activation loop (encoded by exon 17).[17,18] Unlike GISTs, the common primary activating mutations in the context of SM, AML, and germ cell tumors are located in the KIT kinase activation loop, such as D816H/V/Y and N822K, and some have been shown to confer imatinib resistance *in vitro* and/or *in vivo*.[19–21] Therefore, new agents capable of overcoming drug resistance conferred by primary or secondary activation loop mutations in KIT have potential therapeutic utility in drug-resistant GISTs, SM, AML, and other tumors.

Flumatinib (formerly HH-GV-678) is a potent BCR-ABL/PDGFR/KIT inhibitor currently undergoing phase III clinical trials for treatment of Philadelphia chromosome-positive CML in China. Our prior data have revealed that ABL and PDGFR-β as well as KIT kinase activities can be potently inhibited by

imatinib (100.9, 201.8, and 361.8 nM, respectively) and flumatinib (1.2, 307.6, 665.5 nM, respectively). In addition, both of them showed only weak inhibition of vascular endothelial growth factor receptor 2/3, SRC, FLT3, RET, epidermal growth factor receptor, and human epidermal growth factor receptor 2. These results confirm that flumatinib is a selective kinase inhibitor for BCR-ABL, PDGFR, and KIT. A previous report from our laboratory indicated that flumatinib outperforms imatinib as a BCR-ABL inhibitor and effectively overcomes imatinib resistance conferred by BCR-ABL point mutations.[22] The aims of the current study were therefore to investigate the efficacy of flumatinib *in vitro* and *in vivo* against imatinib-sensitive and imatinib-resistant KIT mutants.

Materials and Methods

Compounds. Flumatinib mesylate, imatinib mesylate, and sunitinib malate were synthesized and provided by Jiangsu Hengrui Medicine Co., Ltd (Jiangsu, China).

Site-directed mutagenesis. Murine stem cell virus-based retroviral constructs carrying murine–human hybrid WT KIT cDNA or activating mutant D816V (816 Asp→Val) KIT cDNA were generously provided by Michael H. Tomasson (Washington University School of Medicine, St. Louis, MO, USA). Hybrid KIT alleles were generated by fusing in-frame the extracellular and transmembrane regions of murine KIT with the intracellular region of human KIT. It has been shown that replacement of the human extracellular and transmembrane domains of KIT with homologous murine sequences can improve the expression efficiency and rescue the transforming potential of certain KIT mutants in murine cells.[23] Owing to a downstream internal ribosomal entry site–enhanced GFP cassette, KIT alleles would coexpress with enhanced GFP. The KIT point mutations were generated following Protocol 3 of mutagenesis in Molecular Cloning (3rd edition).[24] For deletion and insertion mutagenesis, mutagenic primers were designed to avoid the deleted sequence or harbor the inserted sequence, respectively. All the PCRs above used the high-fidelity Primestar Hot Start DNA Polymerase (Takara, Dalian, China). Other enzymes used in above experiments were also purchased from Takara. The sequences of all mutants in this study were verified by direct sequencing.

Cell culture and retroviral transfection. The IL-3-dependent murine hematopoietic cell line 32D (ATCC, Manassas, VA, USA) was maintained in RPMI-1640 supplemented with 10% FBS and 15% WEHI-3B (ATCC) conditioned medium as the source of murine IL-3. Retroviral preparation and transfection were carried out according to the protocol and guidelines provided by the Nolan Laboratory at Stanford University (Stanford, CA, USA). Retroviral supernatants were obtained 48 h after transfection of plasmids encoding KIT mutants into the Phoenix-Eco packaging cell line with Fugene 6 (Roche Diagnostics, Indianapolis, IN, USA). The 32D cells were infected with viral supernatants, then 48 h later selected for IL-3-independent growth. Cells transfected with WT KIT were selected with 200 ng/mL rmSCF (R&D Systems, Minneapolis, MN, USA).

Cell proliferation assay. Cells (5×10^3) in 200 μL medium with or without IL-3 were incubated with various concentrations of imatinib, flumatinib, or sunitinib in 96-well plates for 72 h in triplicate. We added MTT (Sigma-Aldrich, St. Louis, MO, USA), and cells were incubated for 4 h. A solubilization solution (a solution of the detergent SDS in diluted hydrochloric acid) was added to dissolve the insoluble purple formazan product into a colored solution. The absorbance of this colored solution was quantified by measuring at 570 nm with a reference filter of 650 nm by a spectrophotometer (Molecular Devices, Sunnyvale, CA, USA). Growth inhibition was plotted as the ratio of the average absorbance in drug-treated wells relative to no-drug controls. The IC_{50} values were calculated by the curve-fitting software GraphPad Prism version 5 (GraphPad Software, San Diego, CA, USA).

Western blot analysis. Cell lysates were prepared in SDS lysis buffer (100 mM Tris–HCl [pH 6.8], 2% SDS, 20% glycerol, and 1 mM DTT). Equal amounts of whole cell lysates were separated by SDS-PAGE, and electroblotted onto Immobilon PVDF membranes (Millipore, Bedford, MA, USA). Blots were probed with anti-phospho-KIT (Tyr-703) antibody, anti-phospho-ERK1/2 (Thr202/Tyr204) antibody, and anti-phospho-STAT3 (Tyr-705) antibody (all Cell Signaling Technology, Beverly, MA, USA). The total amounts of KIT, ERK1/2, and STAT3 were probed with anti-KIT antibody (Dako, Glostrup, Denmark), anti-ERK1/2 antibody (Santa Cruz Biotechnology, Santa Cruz, CA, USA), and anti-STAT3 antibody (Cell Signaling Technology), respectively. Immunoactive proteins were visualized using the Immobilon Western enhanced chemiluminescence system (Millipore) and the signals were captured by a digital bioimaging system (Clinx Science Instruments, Shanghai, China).

***In vivo* experiments.** Six-week-old female Balb/cA-nu/nu mice weighing 17–19 g each were purchased from Shanghai SLAC Laboratory Animal Co., Ltd (Shanghai, China), and raised under specific pathogen-free conditions. Each mouse was injected s.c. with 1×10^7 KIT mutant transformed 32D cells in the right flank. Mice were randomized into groups (n = 8–10 per group) and treated by oral gavage with vehicle, imatinib, flumatinib, or sunitinib for the next 14 days.

For pharmacokinetic/pharmacodynamic studies, mice implanted with 32D-V559D + Y823D cells were randomized into groups (n = 3–4 per group) when the volume of tumors reached 300–400 mm^3, then were treated by oral gavage with vehicle, imatinib, flumatinib, or sunitinib. Peripheral blood was taken from animals into heparinized tubes and plasma was then prepared and stored at −80°C until analysis. After the mice were killed, the tumors were excised, weighed, snap frozen in liquid nitrogen, and stored at −80°C until analyzed. Concentrations of imatinib, flumatinib, and sunitinib in plasma and tissue were determined by HPLC/tandem mass spectrometry following reported procedures.[25]

Animal experiments were carried out in accordance with the Institutional Animal Care and Use Committee guidelines at the Shanghai Institute of Materia Medica (Chinese Academy of Sciences, Shanghai, China).

Statistical analysis. Survival curves were plotted using the Kaplan–Meier method. Between-group differences were analyzed by the log–rank test. All statistical analyses were carried out using GraphPad Prism version 5 (GraphPad Software). $P < 0.05$ was considered statistically significant.

Molecular docking. The crystallographic structure of KIT complexed with imatinib (PDB entry 1t46) was downloaded from the RCSB Protein Data Bank (available at www.pdb.org). More detailed information about molecular docking is provided in Document S1.

Results

Clinically relevant KIT mutants transform 32D cells to IL-3-independent growth and are constitutively activated in these cells. The IL-3-dependent murine cell line 32D was transfected by retroviral vectors expressing WT KIT or 1 of 17 KIT mutants

and selected for IL-3-independent growth. These transforming primary mutations mapped to the extracellular domain (Del [T417Y418D419] ins Ile, and Y503-F504 ins AY),[6,18] the juxtamembrane region (encoded by exon 11) (V559D, Del [V559V560], D579-H580 ins IDPTQLPYD),[2] or activation loop of the kinase domain (D816H/V/Y, and N822K).[5,7] Considering that GISTs with KIT exon 11 mutants commonly become imatinib-resistant due to acquisition of secondary mutations in the kinase domain (i.e., V654A, T670I, D816H, D820G, N822K, Y823D, and A829P),[13,18] we constructed imatinib-resistant double mutants by introducing each of these secondary mutations into the imatinib-sensitive mutant V559D. All of these mutants transformed 32D cells to IL-3-independent growth in the absence of rmSCF, and WT KIT transformed 32D cells to rmSCF-dependent growth. As expected, all transformed cells were GFP positive (data not shown). The 32D cells transformed by any of the KIT mutants showed constitutive phosphorylation of KIT and downstream signaling effectors ERK1/2 and STAT3 (Fig. 1). Consistent with a previous study,[19] we observed differential phosphorylation of two KIT bands of approximately 160 and 145 kDa, representing the fully glycosylated cell surface receptor, and incompletely processed internalized forms of KIT, respectively.

Flumatinib has a selective inhibition pattern toward imatinib-resistant KIT mutants associated with GISTs. Next, we examined the antiproliferative activities of imatinib, sunitinib, and flumatinib against these transformed 32D cell lines. The 32D-V559D or 32D-Del (V559V560) cells were highly sensitive to imatinib, flumatinib, and sunitinib with IC_{50} values of 2–4 nM (Table 1). Those 32D cells expressing Y503-F504 ins AY, which is a typical exon 9 mutant in GISTs, were relatively resistant to both imatinib and flumatinib (IC_{50} values, 192.0 and 275.0 nM, respectively); in contrast, this mutant was sensitive to sunitinib (IC_{50}, 10.9 nM; Table 1). Notably, 32D-(Y503-F504 ins AY) cells showed a drug response pattern closely resembling that of ligand-dependent cell growth (IC_{50} values, 351.8, 517.6 and 16.3 nM for imatinib, flumatinib, and sunitinib, respectively; Table 1). Imatinib, flumatinib, and sunitinib all showed low potency against 32D cells grown in the presence of IL-3 (IC_{50} values >5000 nM; Table 1), indicating a substantial selectivity for inhibition of KIT-transformed cells.

As expected, 32D cells transformed by those double mutants harboring secondary mutations in KIT were resistant to imatinib in varying degrees (IC_{50} values, 50–6552 nM; Table 1). The 32D cells expressing double mutants harboring secondary mutations in the drug/ATP binding pocket, such as V559D + V654A and V559D + T670I, were highly sensitive to sunitinib (IC_{50} values, 3.0 and 2.0 nM, respectively); however, those cells expressing double mutants with secondary activation loop mutations, such as V559D + N822K, V559D + Y823D, and the others, were insensitive to sunitinib (IC_{50} values, 80–704 nM; Table 1). In contrast, 32D-V560D + V654A and 32D-V560D + T670I cells were resistant to flumatinib (IC_{50} values, 99.0 and 419.2 nM, respectively), whereas cells harboring secondary activation loop mutations were relatively sensitive to flumatinib (IC_{50} values, 11.2, 10.4, 6.3, and 11.2 nM for V559D + D820G, V559D + N822K, V559D + Y823D, and V559D + A829P, respectively; Table 1). Despite that 32D-V559D+D816H cells remained ~25-fold more resistant to flumatinib than 32D-V559D cells, 32D-V559D + D816H cells were still more sensitive to flumatinib than imatinib or sunitinib.

The effects of flumatinib on the activation of KIT mutants and downstream signaling pathways were then investigated. In 32D-V559D cells, imatinib, flumatinib, and sunitinib treatment all effectively abolished the phosphorylation of KIT, ERK1/2, and STAT3 (Fig. 2), showing substantial shutdown of the KIT and downstream signaling pathways. In 32D-V559D + Y823D cells, the phosphorylation levels of KIT, ERK1/2, and STAT3 were strongly inhibited by flumatinib, but not imatinib or sunitinib (Fig. 2). Similar findings were observed in 32D-V559D + N822K and 32D-V559D + A829P cells (Fig. S1). The phosphorylation levels of these KIT mutants, as well as ERK1/2 and STAT3, were dose-dependent on each drug over a wide concentration range (1–1000 nM) and correlated with inhibition of cell growth. These results collectively show that flumatinib is capable of overcoming the imatinib and sunitinib resistance conferred by certain secondary activation loop mutations *in vitro*. We previously showed that flumatinib inhibits the tyrosine kinase activity of ABL 80-fold more effectively than imatinib in an ELISA (100.9 and 1.2 nM for imatinib and flumatinib, respectively). Furthermore, these ELISA results correlate with those from our previous cell-based proliferation assays.[22] Given that our proliferation assays were all based on the same 32D cell line, we could exclude the possibility that the enhanced antiproliferative activity of flumatinib is presumably due to increased intracellular flumatinib concentrations. Taken together, our findings suggest that the enhanced

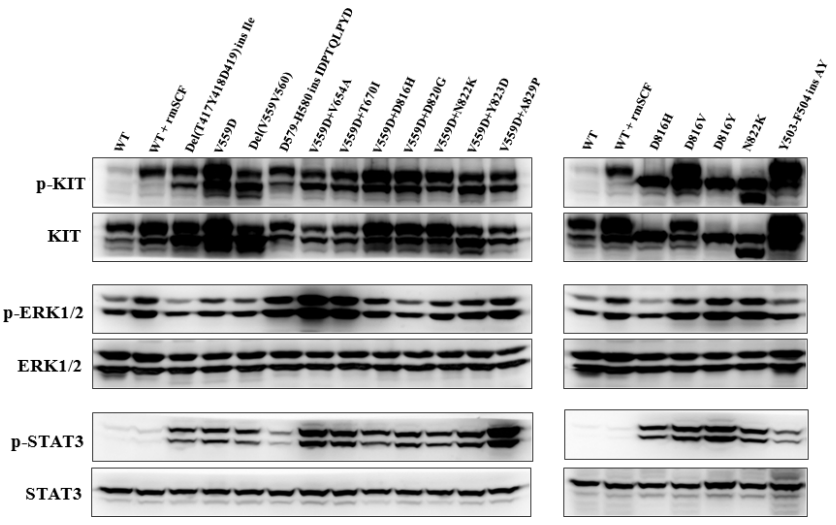

Fig. 1. KIT mutants, downstream signaling effectors ERK1/2, and signal transducer and activator of transcription-3 (STAT3), are constitutively phosphorylated in transformed 32D cell lines. Total cell lysates were analyzed by Western blotting, and the levels of phosphorylated (p-) and total proteins were determined using specific antibodies. rmSCF, recombinant mouse stem cell factor; WT, wild-type.

Table 1. Comparative effects of imatinib, flumatinib, and sunitinib on the proliferation of 32D cell lines expressing transforming KIT mutants

Cell line	Mean ± SD (nM)		
	Imatinib	Flumatinib	Sunitinib
WT + mIL3	>10000	>5000	>10000
WT + rmSCF	351.8 ± 30.6	517.6 ± 110.0	16.3 ± 6.1
Del(T417Y418D419) ins Ile	32.9 ± 11.9	6.3 ± 1.1	7.4 ± 3.1
Y503-F504 ins AY	192.0 ± 9.2	275.0 ± 36.9	10.9 ± 1.4
V559D	3.0 ± 0.5	4.3 ± 0.9	2.0 ± 0.3
Del(V559V560)	2.9 ± 0.6	4.2 ± 1.2	2.8 ± 0.7
D579-H580 ins IDPTQLPYD	59.0 ± 6.3	76.4 ± 4.5	47.4 ± 7.3
V559D+V654A	108.5 ± 14.8	99.0 ± 28.8	3.0 ± 0.5
V559D+T670I	6552 ± 354.5	419.2 ± 48.0	2.0 ± 0.3
D816H	208.8 ± 48.7	34.4 ± 11.8	17.5 ± 3.9
D816V	8585 ± 600.4	1792 ± 451.2	294.7 ± 121.9
D816Y	1046 ± 229.9	302.7 ± 28.6	73.1 ± 21.4
V559D + D816H	963.4 ± 340.9	109.0 ± 43.5	704.4 ± 255.9
V559D+D820G	50.0 ± 9.1	11.2 ± 5.1	80.7 ± 16.8
N822K	252.5 ± 33.1	16.5 ± 5.1	37.0 ± 6.1
V559D + N822K	67.4 ± 30.4	10.4 ± 3.9	112.9 ± 60.9
V559D + Y823D	219.8 ± 48.5	6.3 ± 2.3	579.0 ± 160.3
V559D + A829P	92.4 ± 15.0	11.2 ± 4.1	192.6 ± 36.1

Cells were plated in 96-well plates and incubated with different concentrations of each drug for 72 h in triplicate. Cell proliferation was determined using the MTT assay. Values represent the means ± SDs of at least three independent experiments. mIL-3, mouse interleukin 3; rmSCF, recombinant mouse stem cell factor; WT, wild-type.

antiproliferative activity of flumatinib against 32D cells transformed by certain KIT double mutants is because of its increased inhibitory activity against the kinase activation of these KIT mutants.

It is generally thought that all the primary mutations in exon 11 (encoding the juxtamembrane region) are sensitive to imatinib, and that underlies the clinical successes of imatinib for treatment of most GISTs. However, in our study, 32D cells transformed by D579-H580 ins IDPTQLPYD, a typical exon 11 insertion mutation, showed modest resistance to imatinib, flumatinib, and sunitinib (59.0, 76.4, and 47.4 nM, respectively; Table 1), and that may have implications for the drug responsiveness of GISTs with this type of mutation.

Flumatinib prolongs the survival time of mice implanted with 32D-V559D + Y823D cells. Furthermore, we evaluated the *in vivo* efficacy of imatinib, flumatinib, and sunitinib in a survival model in which 32D-V559D or 32D-V559D + Y823D cells were injected s.c. into Balb/cA-nu/nu mice. As shown in Figure 3 (Kaplan–Meier plots), the median survival time for vehicle-treated mice implanted with 32D-V559D cells was 26.5 days. Oral treatments with imatinib (150 mg/kg, q.d. and b.i.d.), flumatinib (75 mg/kg, q.d. and b.i.d.), and sunitinib (50 mg/kg, q.d.) for 14 days prolonged the median survival to 31.5 (imatinib, q.d.; $P < 0.001$), 36.5 (imatinib, b.i.d.; $P < 0.001$), 30.5 (flumatinib, q.d.; $P < 0.05$), 33.5 (flumatinib, b.i.d.; $P < 0.001$), and 32.5 days ($P < 0.001$) (Fig. 3), respectively, suggesting that all three drugs are effective against 32D-V559D cells *in vivo*.

For mice implanted with 32D-V559D + Y823D cells, the median survival time for vehicle-treated mice was 22 days. Oral treatments with imatinib (150 mg/kg, q.d.) and sunitinib (50 mg/kg, q.d.) for 14 days had no beneficial effects, and even shortened median survival to 20 days (Fig. 3), suggesting that 32D-V559D + Y823D cells are refractory to both imatinib and sunitinib *in vivo*. In contrast, treatments with imatinib (150 mg/kg, b.i.d.) and flumatinib (75 mg/kg, q.d. and b.i.d.) extended the median survival to 23.5 ($P = 0.23$), 25.5 ($P = 0.061$), and 25.5 ($P < 0.05$) days, relative to the vehicle-treated group, respectively (Fig. 3). In addition, the survival of mice treated with flumatinib (75 mg/kg, b.i.d.) was significantly improved compared with mice treated with imatinib (150 mg/kg, q.d.; $P < 0.01$) or sunitinib (50 mg/kg, q.d.; $P < 0.01$).

Tumors derived from these transformed 32D cell lines seemed to be highly metastatic and malignant in nude mice, and could not grow large enough (usually less than 400 mm^3) to ensure accuracy and comparability of the tumor size before they killed their hosts. Therefore, we could not evaluate and compare the efficacy of these antitumor drugs by assessing their effects on the size of tumors in nude mice. Additionally, compared with the vehicle group, flumatinib did not show significant adverse effects on the body weight of mice in the above experiments (Fig. S2).

Pharmacokinetic and pharmacodynamic properties of imatinib, flumatinib, and sunitinib in the xenograft model. To determine the PK and PD relationship in tumors, mice bearing 32D-V559D + Y823D tumors were treated with a single dose of imatinib (150 mg/kg), flumatinib (75 mg/kg), or sunitinib

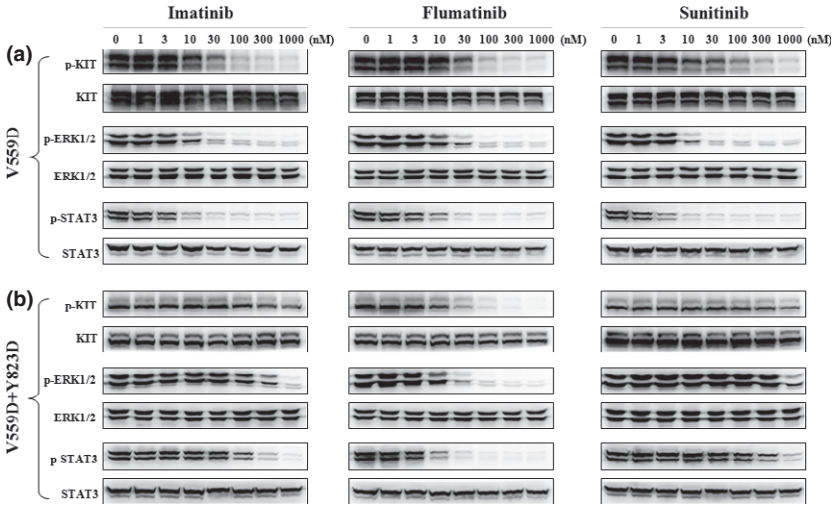

Fig. 2. Effects of imatinib, flumatinib, and sunitinib on the phosphorylation of KIT, ERK1/2, and signal transducer and activator of transcription-3 (STAT3) in 32D-V559D (a) and 32D-V559D+Y823D (b) cells. Cells were grown in the indicated concentration of each drug for 4 h and total cell lysates were analyzed by Western blotting.

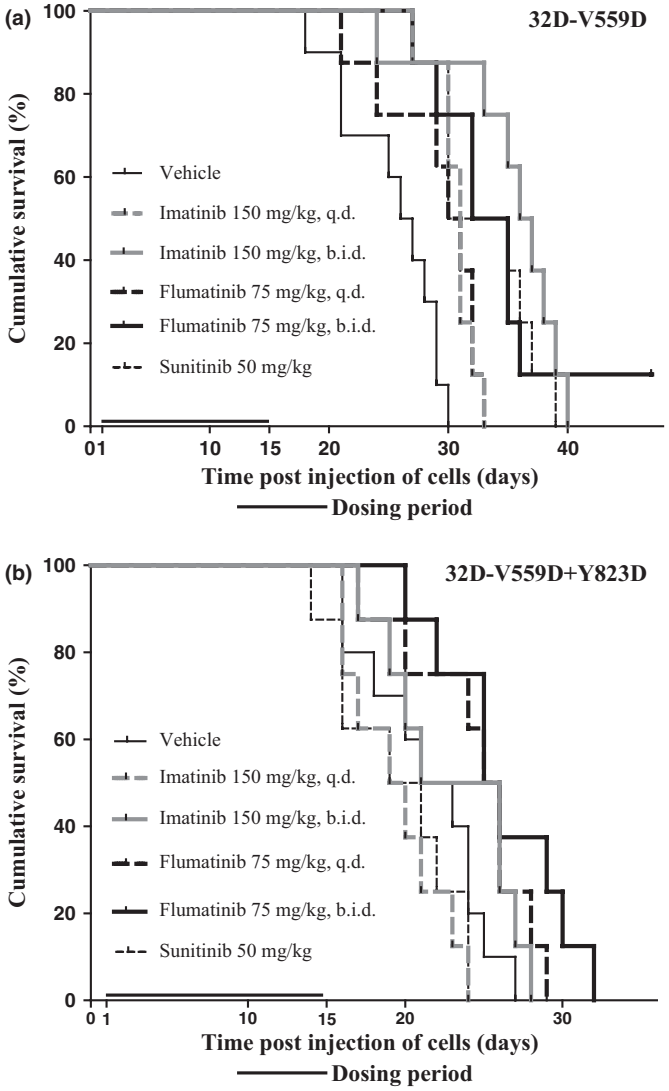

Fig. 3. *In vivo* effects of imatinib, flumatinib, and sunitinib on the survival of mice after s.c. injection of 32D-V559D (a) or 32D-V559D+Y823D (b) cells. Animals were randomized into groups and treated by oral gavage with vehicle, imatinib, flumatinib, or sunitinib according to the indicated dosage regimen and dosing period.

(50 mg/kg). Plasma and tumors were harvested after 1, 2, 4, 8, 12, and 24 h and analyzed for drug concentrations and effects on target efficacy biomarkers.

At 1 h after dosing, the plasma concentration of imatinib achieved 37 483 ng/mL (or 75.94 μM), and the intratumoral imatinib level reached 38 857 ng/g (or 78.72 μM) (Fig. 4a). Thereafter, plasma and intratumoral imatinib concentrations decreased gradually over time (Fig. 4a). These results indicate that imatinib was rapidly absorbed after given orally and achieved peak plasma and intratumoral levels in less than 1 h. In contrast, the plasma flumatinib concentration was highest 2 h after dosing (1073 ng/mL or 1.91 μM), and the intratumoral flumatinib level was highest 4 h after dosing (2721 ng/g or 4.84 μM) (Fig. 4b). For sunitinib, the highest plasma and intratumoral concentrations were achieved 2 and 4 h after dosing, respectively (1098 ng/mL or 2.76 μM, and 21 904 ng/g or 54.97 μM for plasma and tumor, respectively) (Fig. 4c). Intriguingly, our PK data showed that all three agents tended to distribute to the tumors, and this was particularly pronounced for flumatinib and sunitinib (Fig. 4a–c).

To investigate the relationship between time course of drug levels and inhibition of target kinase signaling in tumors, 32D-V559D + Y823D tumors harvested after 2, 4, 8, 12, and 24 h were analyzed using Western blotting for drug effects on phosphorylation levels of KIT and its downstream effectors. Imatinib significantly inhibited the phosphorylation of KIT and STAT3 at 12 h after dosing, however, the phosphorylation of STAT3 restored after 24 h (Fig. 4d), suggesting that a single dose of 150 mg/kg imatinib cannot exert a durable effect. In contrast, the phosphorylation levels of KIT and STAT3 were effectively blocked at 8 h after dosing of 75 mg/kg flumatinib and remained inhibited after 24 h (Fig. 4e). For sunitinib, the phosphorylation levels of KIT and STAT3 were not obviously reduced after dosing with 50 mg/kg sunitinib (Fig. 4f), indicating that V559D + Y823D tumor was still resistant to sunitinib *in vivo*. Unexpectedly, ERK1/2 was constitutively phosphorylated in all tumors.

Flumatinib also effectively overcomes imatinib resistance of certain primary activation loop mutants associated with SM, AML, and germ cell tumors. In addition, some transforming primary activation loop mutations, such as D816H/V/Y and N822K, are frequently observed in SM, AML, and germ cell tumors.[5,7,26,27] Considering that flumatinib may be a potential therapeutic agent against these diseases, we assessed the activity of flumatinib against cell proliferation driven by KIT with these primary mutations. As shown in Table 1, 32D-D816V and 32D-D816Y cells were highly resistant to imatinib, flumatinib, and sunitinib (IC_{50} values, 73.1–8585 nM). The 32D-D816H and 32D-N822K cells were also highly resistant to imatinib (IC_{50} values, 208.8 and 252.5 nM, respectively), but obviously more sensitive to flumatinib (IC_{50} values, 34.4 and 16.5 nM, respectively) or sunitinib (IC_{50} values, 17.5 and 37.0 nM, respectively; Table 1). Furthermore, the phosphorylation levels of D816H and N822K mutants, as well as ERK1/2 and STAT3, were dose-dependent on each drug and correlated with the data from cell proliferation assays (Fig. S3, Table 1). Collectively, these results suggest that flumatinib can effectively overcome the imatinib resistance of D816H and N822K KIT mutants *in vitro*.

Intriguingly, 32D cells transformed by Del(T417Y418D419) ins Ile, which represents a set of extracellular mutations mostly associated with AML, were moderately resistant to imatinib (IC_{50}, 32.9 nM), but clearly sensitive to flumatinib (IC_{50}, 6.3 nM) and sunitinib (IC_{50}, 7.4 nM; Table 1).

Molecular docking model of KIT/flumatinib complex suggests a special mechanism underlying the better performance of flumatinib over imatinib. The crystal structure of KIT/imatinib complexes revealed that imatinib forms four hydrogen bonds with the residues Asp^{810}, Glu^{640}, Thr^{670} and Cys^{673} in the kinase domain, respectively.[28] The main difference between imatinib and flumatinib is that a hydrogen atom in the former is substituted by a trifluoromethyl group in the latter (Fig. 5). To explore the molecular mechanism of imatinib resistance induced by secondary mutations in the KIT kinase domain, we analyzed the structure of the KIT/imatinib complex further. Considering that V654 is spatially proximate to imatinib and T670 forms a hydrogen bond with imatinib, we speculate that the secondary mutations in the drug/ATP binding site are likely to mediate imatinib resistance through steric factors and /or hydrogen bond disrupture (Fig. S4A); however, activation loop mutations do not seem to interact with imatinib directly, which suggests that these mutations may lead to imatinib

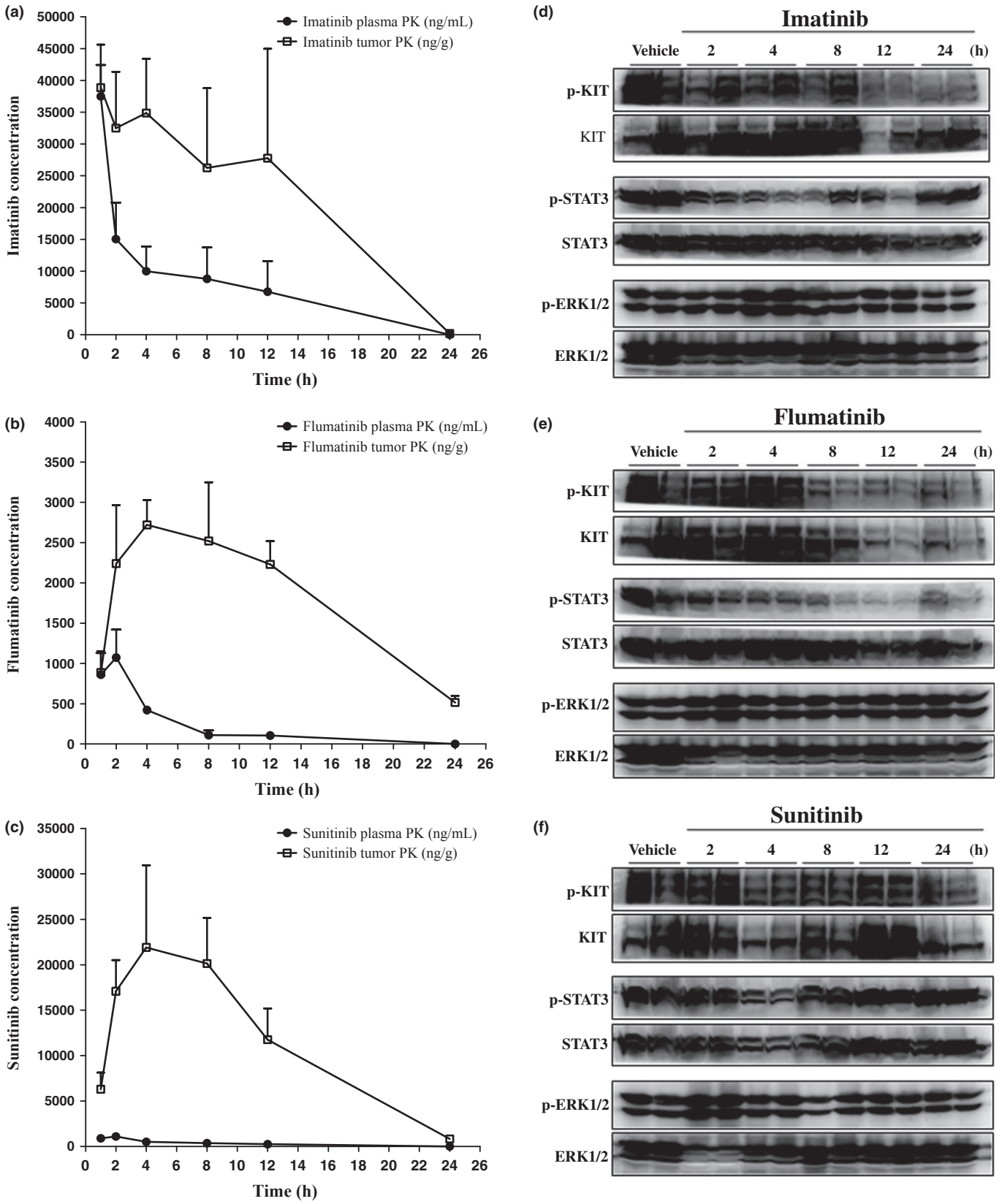

Fig. 4. Pharmacokinetic (PK) and pharmacodynamic properties of imatinib, flumatinib, and sunitinib. Mice bearing 32D-V559D + Y823D tumors received a single dose of 150 mg/kg imatinib, 75 mg/kg flumatinib, or 50 mg/kg sunitinib. Mice were killed at different times post-dosing as indicated and the concentrations of imatinib (a), flumatinib (b), and sunitinib (c) were determined in blood plasma and tumor tissue. The phosphorylation levels of KIT, ERK1/2, and signal transducer and activator of transcription-3 (STAT3) in tumors at various times after dosing of imatinib (d), flumatinib (e), sunitinib (f) were determined by Western blotting.

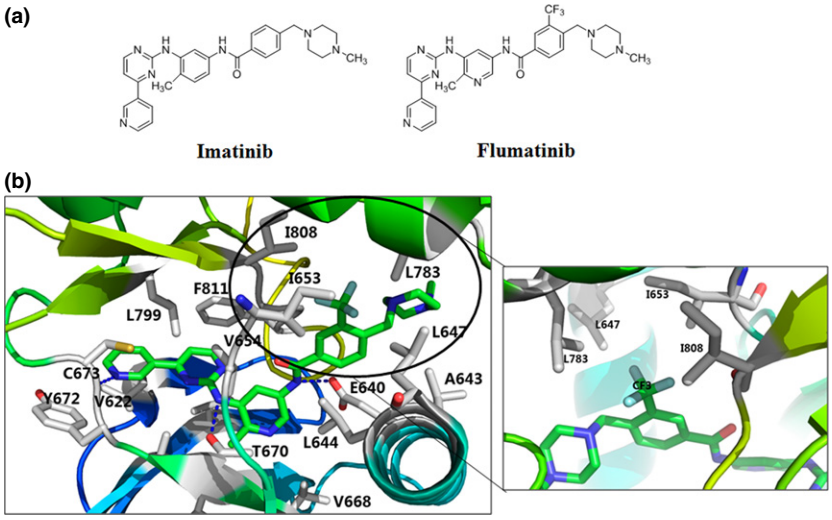

Fig. 5. Molecular modeling of the interactions between flumatinib and KIT kinase domain. (a) Structures of imatinib and flumatinib. (b) Molecular docking model of the KIT/flumatinib complex.

resistance though different mechanisms. To understand the differential effects of flumatinib on the kinase activation of imatinib-resistant KIT double mutants, a molecular model was constructed from the coordinates of the crystal structure of the KIT/imatinib complex, and flumatinib was docked into the imatinib binding site. This docking model suggests that flumatinib locates in the same position and forms the same hydrogen bond interactions with the kinase domain as imatinib (Fig. S4B). Furthermore, the trifluoromethyl group of flumatinib seems to form additional interactions (van der Walls and/or hydrophobic interactions) with a hydrophobic pocket formed by side chains of residues Leu^{647}, Ile^{653}, Leu^{783}, and Ile^{808} in the kinase domain (Fig. 5), and this indicates that flumatinib stands a good chance of having a higher affinity for the kinase domain. This hydrophobic pocket seems to be very important for the kinase activity, because substitution of any one of the four amino acids to an Ala destroys the transformation potential of KIT activating mutants (data not shown).

Discussion

Previous clinical studies have revealed that secondary KIT mutations in patients with imatinib-resistant GISTs tended to cluster in the drug/ATP binding pocket or the kinase activation loop.[12–14,18,29] Heinrich *et al.*[13] summarized the spectrum and frequency of secondary KIT mutations in published reports. Although the secondary mutations seemed to be nonrandom and involved either the ATP binding pocket (V654A, T670I) or the activation loop (C809G, D816H, D820A/E/G, N822K/Y, Y823D), we still could not determine which location (ATP binding pocket or activation loop) is more favored by imatinib-resistant GISTs. Among these mutations, V654A is a frequently occurring gatekeeper mutation, whereas Y823D is a typical activation loop mutation of KIT kinase in the clinical setting. In the current study, these secondary mutations were coexpressed with a common primary mutation (V559D), which recreated the situation often observed in GISTs that show secondary imatinib resistance. Consistent with previous *in vitro* studies, we found that sunitinib potently inhibits the kinase activity of KIT mutants containing secondary mutations in the drug/ATP binding pocket, such as V654A and T670I, but is relatively ineffective at inhibiting KIT mutants harboring secondary mutations in the activation loop.[18] In this report, we characterized flumatinib as a KIT inhibitor that can effectively overcome imatinib and sunitinib resistance of certain KIT mutants with secondary activation loop mutations, both *in vitro* and *in vivo*. Additionally, cell proliferation assays revealed that flumatinib induces very similar effects to imatinib against 32D cells expressing KIT mutants with the exon 11 mutations such as V559D and Del (V559V560), and these findings were confirmed in the *in vivo* efficacy studies in which both drugs significantly prolonged the survival of mice bearing 32D-V559D tumors. For the 32D-V559D survival model, all three kinase inhibitors increased survival by 20–40% over vehicle. In contrast, in the V559D + Y823D model, imatinib and flumatinib increased survival by 6.8% and 16%, respectively, and only the flumatinib effect was statistically significant. Although statistically significant, the *in vivo* effects of these drugs seemed minor in comparison to their *in vitro* results, and further investigations are warranted to explain this discrepancy. Consistent with our previous *in vivo* data, flumatinib was very well tolerated in mice and showed no obvious adverse effects on body weight. Taken together, our findings suggest that flumatinib may be a promising therapeutic agent for patients with KIT-positive GISTs, particularly those for whom prior imatinib therapy failed and disease progressed as a result of KIT secondary activation loop mutations.

Pharmacokinetic and PD studies were carried out to determine whether the *in vivo* effects of imatinib, flumatinib, and sunitinib are correlated with inhibition of target kinase signaling in tumors. Our PK results of imatinib suggest that imatinib has excellent oral bioavailability, which is consistent with clinical PKs of imatinib.[30] Although intratumoral imatinib concentrations achievable after a single dose of 150 mg/kg imatinib are very high and far above concentrations required to actively suppress 32D-V559D + Y823D cell proliferation and inhibit the phosphorylation of V559D + Y823D mutant *in vitro*, our PD studies revealed that they are still insufficient to block KIT signaling effectively and durably in the 32D-V559D + Y832D tumor for a beneficial effect *in vivo*. Further investigations are needed to explain the apparent discrepancy between the *in vitro* and *in vivo* imatinib concentrations required to effectively inhibit KIT kinase activity in 32D-V559D + Y823D cells. In contrast, the PKs of flumatinib suggest that flumatinib has lower oral bioavailability than imatinib. Despite lower intratumoral concentrations, flumatinib

still elicited a more profound and long-lasting PD response than imatinib in tumor tissue following a single oral dose of 75 mg/kg in mice bearing 32D-V559D + Y823D tumors, suggesting that flumatinib concentrations achieved in tumors are sufficient to exert a therapeutic effect against cells expressing this imatinib- and sunitinib-resistant mutant. For sunitinib, although the highest intratumoral concentration achieved 54.97 μM at 4 h after dosing, it did not produce an obvious pharmacodynamic response, which explains why a single oral dose of 50 mg/kg sunitinib did not help the survival of mice implanted with 32D-V559 + Y823D cells. In addition, the sunitinib plasma concentrations were much lower than that in tumors, which is consistent with previous clinical findings that sunitinib has a large volume of distribution about 2230 L.[31]

Interestingly, there is a discrepancy between the PK behavior and PD effects of imatinib and flumatinib. Both drugs reached high intratumoral concentrations at 4 h, and yet there were no reductions in phosphorylation of KIT. It seemed that the inhibitory effects of imatinib or flumatinib on KIT activation in tumors were delayed. In contrast, and consistent with our *in vitro* data, the phosphorylation levels of STAT3 were more sensitive to drug treatments and probably more accurately reflected the inhibition of target kinase signaling. The apparent discrepancy between the *in vitro* and *in vivo* findings in the transformed 32D cells may reflect incomplete KIT pathway inactivation *in vivo*. Indeed, ERK1/2 was constitutively activated in all tumors and its phosphorylation status did not vary with that of KIT or STAT3, suggesting that alternative growth factor or cytokine signaling pathways are activated *in vivo*.

Additionally, we also simultaneously evaluated the effectiveness of other KIT inhibitors including nilotinib, dasatinib, sorafenib, and cabozantinib, against the proliferation of these 32D cell lines transformed by various KIT mutants (Table S1). Nilotinib is a second generation inhibitor of the BCR-ABL tyrosine kinase that also inhibits the kinase activity of KIT and also has a trifluoromethyl group at a similar position as flumatinib. Although nilotinib has clinical activity in imatinib- and sunitinib-resistant GISTs,[32] the effects of nilotinib on various KIT mutations found in GISTs remain poorly defined. Here, our findings revealed that nilotinib can inhibit the proliferation of 32D cells harboring secondary activation loop mutations more effectively than imatinib, and that may underlie the clinical activity of nilotinib in imatinib- and sunitinib-resistant GISTs. Some previous studies have reported the *in vitro* potency of dasatinib against certain imatinib-resistant KIT mutants.[33,34] Here, our more complete *in vitro* results of dasatinib indicate that this inhibitor can effectively inhibit almost all KIT mutants except the one with the secondary gatekeeper mutation T670I. Recently, sorafenib has been reported to have superior *in vitro* potency compared with imatinib and sunitinib against a panel of GIST-related drug-resistant KIT mutants (as assessed by biochemical IC_{50}).[35] Overall, our *in vitro* results of sorafenib are consistent with those. Cabozantinib is a small molecule inhibitor of multiple kinases including KIT. Here, for the first time, our results suggest that cabozantinib has high *in vitro* potency against most drug-resistant KIT mutants. These results have implications for the further development of treatments for drug-resistant GISTs.

It has been proposed that KIT mutations in the juxtamembrane region result in the constitutive activation of the tyrosine kinase by compromising the inhibitory function of the juxtamembrane.[36] However, activating mutations in the activation loop seem to predispose the mutated kinase in an active conformation which is resistant to both imatinib and sunitinib, and it has been proposed that it is the conversion from the drug-favorable unactivated kinase conformation to the drug-insensitive active form that results in loss of inhibition.[17] Based on this hypothesis, we speculate that flumatinib still could effectively bind the active conformation and inhibit the kinase activation because of the additional van der Walls and/or hydrophobic interactions between the trifluoromethyl group of flumatinib and the hydrophobic pocket of the kinase domain, and that may be the reason for increased drug sensitivity of the imatinib-resistant active conformation to inhibition by flumatinib. Similar mechanisms have been proposed to underlie the enhanced activity of a series of inhibitors with the trifluoromethyl group against the kinase activity of ABL.[37–39]

The favorable effectiveness, both *in vitro* and *in vivo*, and PK/PD properties of flumatinib provide a reliable rationale for the clinical evaluation of this drug in imatinib-resistant malignancies. Moreover, the relationships between mutations and drug sensitivity/resistance defined in our cell-based model provide a rationale for patient selection for single-agent therapy.

Acknowledgments

This work was supported by research funding from the National Natural Science Foundation of China (Grant Nos. Y201181042 and 81273546) and from the National Science and Technology Major Project "Key New Drug Creation and Manufacturing Program", China (Grant Nos. 2013ZX09102008 and 2013ZX09402102-001-004).

Disclosure Statement

The authors have no conflict of interest.

Abbreviations

b.i.d.	twice a day
GIST	gastrointestinal stromal tumor
IL-3	interleukin-3
PDGFR	platelet-derived growth factor receptor
PD	pharmacodynamic
PK	pharmacokinetic
q.d.	once a day
rmSCF	recombinant mouse stem cell factor
SM	systemic mastocytosis
STAT3	signal transducer and activator of transcription-3
WT	wild-type

References

1 Hirota S, Isozaki K, Moriyama Y *et al.* Gain-of-function mutations of KIT in human gastrointestinal stromal tumors. *Science* 1998; **279**: 577–80.
2 Rubin BP, Singer S, Tsao C *et al.* KIT activation is a ubiquitous feature of gastrointestinal stromal tumors. *Cancer Res* 2001; **61**: 8118–21.
3 Corless CL, Fletcher JA, Heinrich MC. Biology of gastrointestinal stromal tumors. *J Clin Oncol* 2004; **22**: 3813–25.
4 Longley BJ, Tyrrell L, Lu S-Z *et al.* Somatic KIT activating mutation in urticaria pigmentosa and aggressive mastocytosis: establishment of clonality in a human mast cell neoplasm. *Nat Genet* 1996; **12**: 312–14.
5 Longley BJ Jr, Metcalfe DD, Tharp M *et al.* Activating and dominant inactivating KIT catalytic domain mutations in distinct clinical forms of human mastocytosis. *Proc Natl Acad Sci* 1999; **96**: 1609–14.
6 Gari M, Goodeve A, Wilson G *et al.* KIT proto-oncogene exon 8 in-frame deletion plus insertion mutations in acute myeloid leukaemia. *Br J Haematol* 2001; **105**: 894–900.

7 Jiao B, Wu C, Liang Y *et al.* AML1-ETO9a is correlated with KIT overexpression/mutations and indicates poor disease outcome in t (8; 21) acute myeloid leukemia-M2. *Leukemia* 2009; **23**: 1598–604.
8 Tian Q, Frierson HF, Krystal GW, Moskaluk CA. Activating KIT gene mutations in human germ cell tumors. *Am J Pathol* 1999; **154**: 1643–7.
9 Curtin JA, Busam K, Pinkel D, Bastian BC. Somatic activation of KIT in distinct subtypes of melanoma. *J Clin Oncol* 2006; **24**: 4340–6.
10 Debiec-Rychter M, Sciot R, Le Cesne A *et al.* KIT mutations and dose selection for imatinib in patients with advanced gastrointestinal stromal tumours. *Eur J Cancer* 2006; **42**: 1093–103.
11 Heinrich MC, Corless CL, Demetri GD *et al.* Kinase mutations and imatinib response in patients with metastatic gastrointestinal stromal tumor. *J Clin Oncol* 2003; **21**: 4342–9.
12 Antonescu CR, Besmer P, Guo T *et al.* Acquired resistance to imatinib in gastrointestinal stromal tumor occurs through secondary gene mutation. *Clin Cancer Res* 2005; **11**: 4182–90.
13 Heinrich MC, Corless CL, Blanke CD *et al.* Molecular correlates of imatinib resistance in gastrointestinal stromal tumors. *J Clin Oncol* 2006; **24**: 4764–74.
14 Debiec-Rychter M, Cools J, Dumez H *et al.* Mechanisms of resistance to imatinib mesylate in gastrointestinal stromal tumors and activity of the PKC412 inhibitor against imatinib-resistant mutants. *Gastroenterology* 2005; **128**: 270–9.
15 Maki R, Fletcher J, Heinrich M *et al.* Results from a continuation trial of SU11248 in patients (pts) with imatinib (IM)-resistant gastrointestinal stromal tumor (GIST). *J Clin Oncol* (ASCO Annual Meeting Proceedings, Meeting Abstracts) 2005; **23** (Suppl. 16): 9011.
16 Demetri GD, van Oosterom AT, Garrett CR *et al.* Efficacy and safety of sunitinib in patients with advanced gastrointestinal stromal tumour after failure of imatinib: a randomised controlled trial. *Lancet* 2006; **368**: 1329–38.
17 Gajiwala KS, Wu JC, Christensen J *et al.* KIT kinase mutants show unique mechanisms of drug resistance to imatinib and sunitinib in gastrointestinal stromal tumor patients. *Proc Natl Acad Sci* 2009; **106**: 1542–7.
18 Heinrich MC, Maki RG, Corless CL *et al.* Primary and secondary kinase genotypes correlate with the biological and clinical activity of sunitinib in imatinib-resistant gastrointestinal stromal tumor. *J Clin Oncol* 2008; **26**: 5352–9.
19 Growney JD, Clark JJ, Adelsperger J *et al.* Activation mutations of human KIT resistant to imatinib mesylate are sensitive to the tyrosine kinase inhibitor PKC412. *Blood* 2005; **106**: 721.
20 Ma Y, Zeng S, Metcalfe DD *et al.* The KIT mutation causing human mastocytosis is resistant to STI571 and other KIT kinase inhibitors; kinases with enzymatic site mutations show different inhibitor sensitivity profiles than wild-type kinases and those with regulatory-type mutations. *Blood* 2002; **99**: 1741–4.
21 Pardanani A, Elliott M, Reeder T *et al.* Imatinib for systemic mast-cell disease. *Lancet* 2003; **362**: 535–6.
22 Luo H, Quan H, Xie C, Xu Y, Fu L, Lou L. HH-GV-678, a novel selective inhibitor of BCR-ABL, outperforms imatinib and effectively overrides imatinib resistance. *Leukemia* 2010; **24**: 1807–9.
23 Xiang Z, Kreisel F, Cain J, Colson A, Tomasson MH. Neoplasia driven by mutant KIT is mediated by intracellular, not plasma membrane, receptor signaling. *Mol Cell Biol* 2007; **27**: 267–82.
24 Sambrook J, Russell DW. *Molecular Cloning: A Laboratory Manual* (Chinese version), Chapter 13. Beijing: Cold Spring Harbor Laboratory Press, 2001; 1095–9.
25 Yang Y, Liu K, Zhong D, Chen X. Simultaneous determination of flumatinib and its two major metabolites in plasma of chronic myelogenous leukemia patients by liquid chromatography-tandem mass spectrometry. *J Chromatogr B Analyt Technol Biomed Life Sci* 2012; **895-896**: 25–30.
26 Wang Y-Y, Zhou G-B, Yin T *et al.* AML1-ETO and KIT mutation/overexpression in t (8; 21) leukemia: implication in stepwise leukemogenesis and response to Gleevec. *Proc Natl Acad Sci USA* 2005; **102**: 1104–9.
27 Kemmer K, Corless CL, Fletcher JA *et al.* KIT mutations are common in testicular seminomas. *Am J Pathol* 2004; **164**: 305.
28 Mol CD, Dougan DR, Schneider TR *et al.* Structural basis for the autoinhibition and STI-571 inhibition of KIT tyrosine kinase. *J Biol Chem* 2004; **279**: 31655–63.
29 Wardelmann E, Thomas N, Merkelbach-Bruse S *et al.* Acquired resistance to imatinib in gastrointestinal stromal tumours caused by multiple KIT mutations. *Lancet Oncol* 2005; **6**: 249–51.
30 Peng B, Lloyd P, Schran H. Clinical pharmacokinetics of imatinib. *Clin Pharmacokinet* 2005; **44**: 879–94.
31 Goodman VL, Rock EP, Dagher R *et al.* Approval summary: sunitinib for the treatment of imatinib refractory or intolerant gastrointestinal stromal tumors and advanced renal cell carcinoma. *Clin Cancer Res* 2007; **13**: 1367–73.
32 Montemurro M, Schöffski P, Reichardt P *et al.* Nilotinib in the treatment of advanced gastrointestinal stromal tumours resistant to both imatinib and sunitinib. *Eur J Cancer* 2009; **45**: 2293–7.
33 Schittenhelm MM, Shiraga S, Schroeder A *et al.* Dasatinib (BMS-354825), a dual SRC/ABL kinase inhibitor, inhibits the kinase activity of wild-type, juxtamembrane, and activation loop mutant KIT isoforms associated with human malignancies. *Cancer Res* 2006; **66**: 473–81.
34 Guida T, Anaganti S, Provitera L *et al.* Sorafenib inhibits imatinib-resistant KIT and platelet-derived growth factor receptor β gatekeeper mutants. *Clin Cancer Res* 2007; **13**: 3363–9.
35 Heinrich MC, Marino-Enriquez A, Presnell A *et al.* Sorafenib inhibits many kinase mutations associated with drug-resistant gastrointestinal stromal tumors. *Mol Cancer Ther* 2012; **11**: 1770–80.
36 Tarn C, Merkel E, Canutescu AA *et al.* Analysis of KIT mutations in sporadic and familial gastrointestinal stromal tumors: therapeutic implications through protein modeling. *Clin Cancer Res* 2005; **11**: 3668–77.
37 Azam M, Seeliger MA, Gray NS, Kuriyan J, Daley GQ. Activation of tyrosine kinases by mutation of the gatekeeper threonine. *Nat Struct Mol Biol* 2008; **15**: 1109–18.
38 Duveau DY, Hu X, Walsh MJ *et al.* Synthesis and biological evaluation of analogues of the kinase inhibitor nilotinib as ABL and KIT inhibitors. *Bioorg Med Chem Lett* 2013; **23**: 682–6.
39 Horio T, Hamasaki T, Inoue T *et al.* Structural factors contributing to the ABL/LYN dual inhibitory activity of 3-substituted benzamide derivatives. *Bioorg Med Chem Lett* 2007; **17**: 2712–17.

Supporting Information

Additional supporting information may be found in the online version of this article:

Doc. S1. Supporting information regarding molecular docking.

Fig. S1. Effects of imatinib, flumatinib, and sunitinib on the phosphorylation of KIT, ERK1/2, and signal transducer and activator of transcription-3 (STAT3) in 32D-V559D + N822K and 32D-V559D + A829P cells.

Fig. S2. Effects of imatinib, flumatinib, and sunitinib on the body weight of mice after injection of 32D-V559D or 32D-V559D + Y823D cells.

Fig. S3. Effects of imatinib, flumatinib, and sunitinib on the phosphorylation of KIT, ERK1/2, and signal transducer and activator of transcription-3 (STAT3) in 32D-D816H and 32D-N822K cells.

Fig. S4. Plane diagrams showing the interactions between KIT kinase domain and imatinib/flumatinib.

Table S1. Imatinib, flumatinib, sunitinib, nilotinib, dasatinib, sorafenib, and cabozantinib IC_{50} values of 32D cell lines expressing transforming KIT mutants.